Bioorganic & Medicinal Chemistry 18 (2010) 6197–6207

Contents lists available at ScienceDirect

Bioorganic & Medicinal Chemistry

journal homepage: www.elsevier.com/locate/bmc

Synthesis, and biological evaluation of 2-(4-aminophenyl)benzothiazole derivatives as photosensitizing agents

Wan-Ping Hu [a,c], Yin-Kai Chen [a], Chao-Cheng Liao [f], Hsin-Su Yu [b,c], Yi-Min Tsai [f], Shu-Mei Huang [b], Feng-Yuan Tsai [d], Ho-Chuan Shen [f], Long-Sen Chang [e], Jeh-Jeng Wang [f,*]

[a] Department of Biotechnology, College of Life Science, Kaohsiung Medical University, Kaohsiung, Taiwan
[b] Department of Dermatology, College of Medicine, Kaohsiung Medical University, Kaohsiung, Taiwan
[c] Center of Excellence for Environmental Medicine, Kaohsiung Medical University, Kaohsiung, Taiwan
[d] Division of Environmental Health and Occupational Medicine, National Health Research Institutes, Miaoli, Taiwan
[e] Institute of Biomedical Science, National Sun Yat-Sen University, Kaohsiung, Taiwan
[f] Department of Medicinal and Applied Chemistry, Kaohsiung Medical University, Kaohsiung City 807, Taiwan

ARTICLE INFO

Article history:
Received 24 February 2010
Revised 23 April 2010
Accepted 24 April 2010
Available online 29 April 2010

Keywords:
Photodynamic therapy
2-(4-Aminophenyl)benzothiazoles
UVA
Mitochondria
MAPK
Apoptosis

ABSTRACT

Photodynamic therapy (PDT) employing exogenous photosensitizers is currently being approved for treatment of basal cell carcinoma (BCC). 2-(4-Aminophenyl)benzothiazoles (**6**) consist of chromophoric structure and absorb light in the UVA (315–400 nm). These results encouraged us to design and synthesize a diversity of 2-phenylbenzothiazoles (**6**). Studies on the apoptotic mechanism involved in photosensitive effects induced by UVA-activated **6** in BCC cells are carried out in the present article. **6**-UVA-treated cells displayed several features of apoptosis, including an increase in the sub-G1 population, a significantly increased annexin V binding, and activation of caspase-3. **6**-UVA induced a decrease in mitochondrial membrane potential ($\Delta\psi_{mt}$) and ATP via enhanced ROS generation and promoted phosphorylation of extracellular signal-regulated kinase (ERK) and p38 MAPK expression. These results suggest that **6**-UVA elicits photosensitive effects in mitochondria processes which involve ERK and p38 activation, and ultimately lead to BCC cell apoptosis.

1. Introduction

Nonmelanoma skin cancer (NMSC) is an increasing problem in the world.[1] Basal cell carcinoma (BCC) is the most common type of NMSC, and most frequently occurs in people with fair skin.[2] Photodynamic therapy (PDT), a noninvasive treatment and with excellent cosmetic results, is used for the prevention and treatment of BCC cells.[3–5] It employs a combination of a photosensitizing agent and light.[6] Light activation of a photosensitizer accumulates in the tumor, and in the presence of molecular oxygen, leads to reactive oxygen species (ROS) generation, which ultimately kills the target cells.[7] Nevertheless, reported cure rates vary, and the transdermal penetration levels for both the photosensitizer and its activating light source are listed as limiting factors. These limitations have prompted the research for new photosensitizers.

2-Phenylbenzothiazoles (**A**, Fig. 1) represent a novel class of potent and selective antitumor agents.[8,9] For instance, 2-(4-aminophenyl)benzothiazoles (**6**, Scheme 1) were originally prepared as synthetic intermediates within a programme to design potential tyrosine kinase inhibitors modeled on structural comparisons with the flavone quercetin and the isoflavone genistein, which compete at the ATP-binding sites of tyrosine kinases.[10,11] However, other biological profiles may also be involved in this complicated biological phenomenon and further investigation is needed to address this issue. The synthesis and biological evaluation of **6** was carried out in our laboratory. Due to these compounds having chromophoric structure and light absorption in the UVA range (320–400 nm), this in vitro study analyses the photosensitive effect of UVA-activated **6** in BCC cells. One can speculate that UVA will produce side effects such as carcinogenesis and photoaging, but in our system, these do not appear because the exposure time required for **6** activation was very short and did not lead to chronic exposure to UVA.

Mitochondria are well known to participate actively in the production of ROS which might be harmful if produced excessively,

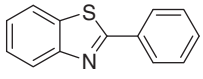

A

Figure 1. Structures of 2-phenyl-benzothiazoles **A**.

* Corresponding author. Tel.: +886 7 312 1101x2275; fax: +886 7 312 5339.
E-mail address: jjwang@kmu.edu.tw (J.-J. Wang).

0968-0896/$ - see front matter © 2010 Elsevier Ltd. All rights reserved.
doi:10.1016/j.bmc.2010.04.082

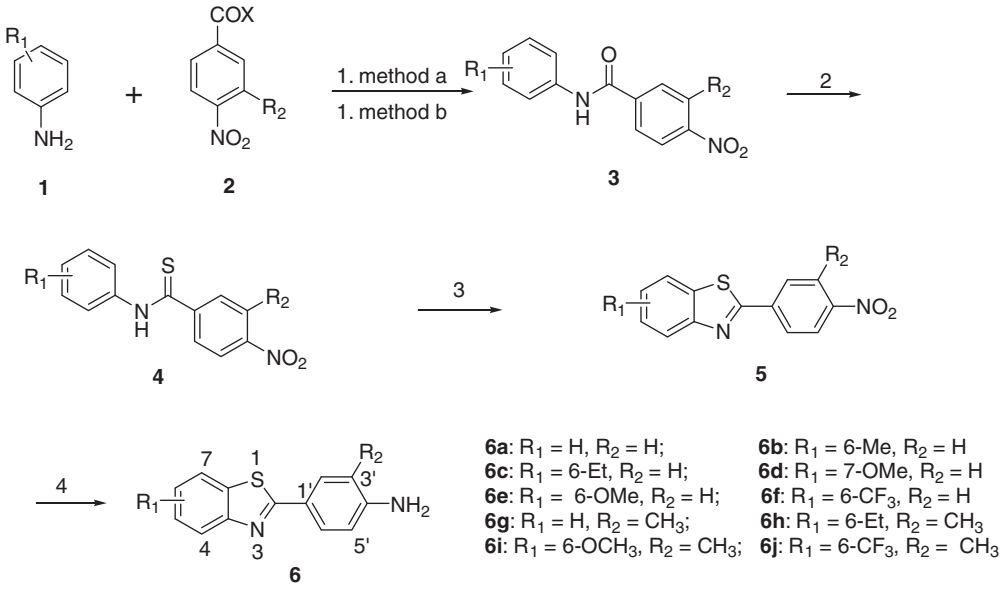

Scheme 1. Total synthesis of 2-(4-aminophenyl)benzothiazoles **6**. Reagents and conditions: (1) method a: X = Cl, pyridine, reflux; method b: X = OH, $SOCl_2$, benzene, reflux. (2) Lawesson's reagent, chlorobenzene, 135 °C. (3) $K_3Fe(CN)_6$ aq, NaOH, 90 °C. (4) H_2/Pd/C 10%, CH_2Cl_2, 25 °C.

and are critically involved in the regulation of cell death pathways.[12] Permeabilization of the mitochondrial outer membrane and subsequent release of proapoptotic proteins from the intermembrane space are viewed as decisive events in the initiation and/or execution of apoptosis.[13] In addition, recent evidence has indicated that ROS play a pivotal role in UVA-induced cell damage.[14] Consequently, cell death induced by UVA-activated **6** might be correlated with mitochondrial depolarization. The mitogen-activated protein kinase (MAPK) family consists of extracellular signal-regulated kinase (ERK), c-Jun N-terminal kinase (JNK), and p38 MAPK. JNK and p38 MAPK pathways are known to be activated by a variety of environmental stresses and chemicals,[15] while the ERK cascade is activated by mitogenic stimuli and is critical for proliferation and survival.[16] However, ERK signaling has been suggested to be proapoptotic in cells undergoing apoptosis.[17,18] In this regard, we have initiated experiments aimed at characterizing the above signaling molecules in the process of apoptosis after BCC cells were treated with **6**-UVA.

The aim of this study was to evaluate the newly synthesized **6** as photosensitizing agents and investigate the apoptotic mechanisms induced by **6**-UVA on BCC cells.

2. Results and discussion

2.1. Syntheses

The preparation of 2-(4-aminophenyl)benzothiazoles **6** is shown in Scheme 1.

4-Nitro-*N*-phenyl benzamides **3** were obtained by the reaction of anilines **1** with nitrobenzoyl chlorides **2** in pyridine under reflux for 4 h (method A). Alternatively, anilines **1** were coupled to nitrobenzoic acids **2** in the presence of thionyl chloride in benzene under reflux condition to give benzamides **3** in high yields (method B). The benzamides **3** were treated with Lawesson's reagent in chlorobenzene under reflux to form 4-nitro-*N*-phenylthiobenzamides **4** in good yields. Cyclization of compound **4** promoted by potassium ferricyanide to produce 2-(4-nitrophenyl)benzothiazoles **5**,[19] followed by catalytic reduction of nitro group of **5** with palladium on charcoal in methanol generated the target compounds **6** in excellent yields.

2.2. Cell viability

The effect of UVA-activated **6** on BCC cell viability was evaluated by MTT assay. BCC cells were treated with different concentrations of **6f** for 4 h followed by 1 J/cm^2 UVA irradiation. Twenty-four hours after exposure, cell viability was determined. As shown in Figure 2A, the inhibitory effect is dependent on drug concentration. At concentrations of 4 μM **6f**, the cell survival was below 50% after 1 J/cm^2 UVA irradiation. To elucidate whether 1 J/cm^2 UVA irradiation is the most effective dosage in this study, cells were pretreated with 4 μM **6f** before UVA treatment. Compared with that of the untreated controls, the cell viability of BCC cells was 71%, 65%, and 45% after irradiation with 0.25, 0.5, and 1 J/cm^2 UVA treatment respectively. In addition, our data also showed that **6**-UVA exhibited a higher inhibitory activity more than either UVA irradiation alone or treatment with exogenous **6** alone, and **6f** alone does not have cytotoxicity against BCC cells (Fig. 2B).

2.3. Cellular sub-G1 accumulation

To investigate the effects of compound 6 on cell cycle progression of BCC cells, the DNA content of cell nuclei was measured by flow cytometric analysis. Agent action resulted in cells having a hypodiploid DNA content (sub-G1 material) that is characteristic of apoptosis and reflects fragmented DNA as shown in Figure 3. BCC cells were treated with 4 μM agents then 1 J/cm^2 UVA irradiation. Twenty-four hours after irradiation, the apoptotic effects in 2.2% (control), 6.5% (**6a**), 13.4% (**6b**), 29.2% (**6c**), 24.4% (**6d**), 6.5% (**6e**), 35.4% (**6f**), 13.6% (**6g**), 13.8% (**6h**), 14.8% (**6i**) and 6.4% (**6j**) of sub-G1 DNA peak were obtained. Because the compound **6f** exhibited the most sub-G1 accumulation on BCC cells, it was selected as a model for further studies.

2.4. Apoptosis detection

Caspase-3 has been shown to be one of the most important cell executioners for apoptosis.[20,21] The expressions of caspase-3 activity were determined using colorimetric assay. Compared with

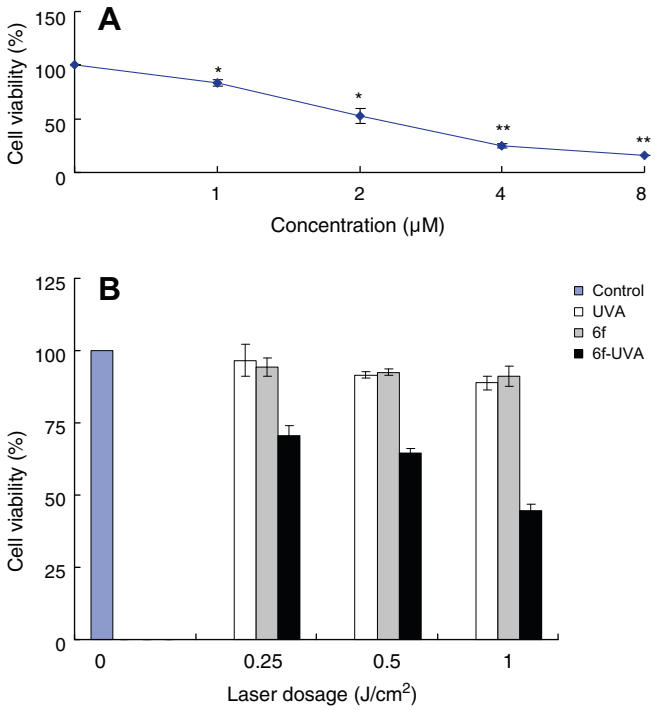

Figure 2. Effect of **6**-UVA cell viability. (A) Dose–response curves for compound **6f** tested against BCC cells. Cells were seeded in a 96-well plate at 2500 cells per well and cultivated overnight until cell attachment. **6f**-UVA at the indicated concentration was added into the culture media in triplicate and incubated for 4 h before 1 J/cm^2 UVA irradiation. Twenty-four hours after irradiation, the MTT reagent was added into each well. The absorbance is directly proportional to the number of living cells. (B) To clarify whether **6**-UVA has more cytotoxicity than either UVA irradiation alone or treatment with **6** alone, cells were cultured with or without 4 μM **6f** before different dosage of UVA irradiation. $^*p$ <0.05, $^{**}p$ <0.01 as compared with the control.

the untreated control group, the caspase-3 activity of BCCs increased after **6f**-UVA treatment (p <0.01) (Fig. 4A). Moreover, treatment of BCC cells with 0, 2, and 4 μM **6f** at 1 J/cm^2 UVA irradiation induced apoptotic cells (annexin V$^+$/PI$^-$) at levels of 0.2%, 19.5%, and 27.5%, respectively. In contrast, there was no obvious change of necrotic cells (annexin V$^+$/PI$^+$) (Fig. 4B). In addition, it would be interesting to know the apoptotic activity of **6f**-UVA on normal cells. Thus, human dermal fibroblast cells were used to clarify this issue. Data from morphology observation and annexin V/PI binding assays showed that no significant apoptotic effect was seen after **6f**-UVA treatment as compared with the control group (Fig. 4C). These results encouraged us to further study the apoptotic mechanism involved in photosensitive effects induced by **6f**-UVA in BCC cells.

2.5. Mitochondrial dysfunction

Growing evidence suggests that mitochondrial dysfunction plays a key role in oxidative stress,[22] which induces production of ROS, and can lead to the apoptotic mode of cell death.[23] To determine whether ROS was involved in **6f**-UVA-induced mitochondria dependent apoptosis, we measured the production of intracellular H_2O_2 using the DCFH-DA probe. Our result showed that **6f**-UVA significantly increases intracellular H_2O_2 levels. In addition, catalase significantly abrogated the increased ROS production of BCC cells treated with 4 μM **6f**-UVA (Fig. 5A). Mitochondrial membrane potential ($\Delta\psi_{mt}$) is an important parameter not only for mitochondrial but also cellular status. A decline of $\Delta\psi_{mt}$ is an early event in the process of cell death. The decrease of fluorescence intensity reflects the collapse of $\Delta\psi_{mt}$, which generally defines an early but already irreversible stage of apoptosis. Therefore, we examined whether the initial ROS generation after **6f**-UVA alters $\Delta\psi_{mt}$. BCC cells were harvested after 0, 2, and 4 μM **6f**-UVA treatment, then analyzed by flow cytometry after $DiOC_6$ dye labeling. The dye binds to the inner and outer membrane of mitochondria and undergoes a red shift in fluorescence during membrane depolarization. As demonstrated in Figure 5B, cells treated with dosages equal to or greater than 2 μM exhibited significant decline of $\Delta\psi_{mt}$ in BCC cells. ATP is the central parameter of cellular energetics, metabolic regulation and cellular signaling; therefore, determination of intracellular ATP is worthwhile in the characterization of cellular physiology. Compared with that of untreated control, the intracellular ATP content of BCC cells decreased about 30% and 45% after 2 and 4 μM of **6f**-UVA treatment, respectively (Fig. 5C).

2.6. Activation of MAPKs pathways

To determine the potential involvement of various protein kinase pathways in **6f**-UVA-induced apoptosis, MAPK activities were evaluated by measuring phosphorylation of MAPK subfamilies. Compared with the untreated control group, the phosphorylation of ERK (p-ERK) and p38 (p-p38) of BCC cells increased after treatment with 6f-UVA at a concentration of 4 μM. In contrast to ERK and p38, treatment of BCC cells with **6f**-UVA did not stimulate the phosphorylation of JNK MAPK (Fig. 6A). Moreover, to elucidate whether the activity of MAPK might be due to the decrease in cellular ATP synthesis, cells were pretreated with oligomycin (a mitochondria-specific F_0F_1 ATP synthase inhibitor) or ATP before 4 μM **6f**-UVA treatment. Our results showed that pretreatment with oligomycin but not ATP increased the ERK activation (Fig. 6B).

3. Conclusions

Previous reports have shown that 2-(4-aminophenyl)benzothiazoles have the potency of growth inhibition activity against cancer cell lines. In this study, we provide evidence indicating that most of the **6**, under UVA light exposure, induced BCC cell apoptosis. This novel finding raised our interest and prompted us to elucidate the signaling mechanism of BCC apoptosis induced by **6**-UVA treatment. We found that when cells were pretreated with **6** for 4 h before 1 J/cm^2 UVA irradiation, **6**-UVA exhibited a cytotoxicity effect on BCCs, and this inhibitory activity is dependent on drug concentration. We hypothesized that the antiproliferative effect of **6**-UVA may be associated with cellular apoptosis. Our results showed that **6**-UVA induces a markedly increased accumulation of sub-G1 phase and triggers apoptosis as revealed by the increased annexin V-FITC cells and the caspase-3 activation.

Many photochemical experiments have indicated that the primary event in any photosensitization process is the absorption of photon energy and the following generation of ROS. Our data indicated that **6f**-UVA promotes H_2O_2 (a representative ROS) generation. In addition, application of catalase (H_2O_2 scavenger) abrogated the enhanced ROS of BCC cells treated with **6f**-UVA. Because mitochondria are known to be a significant source of ROS and $\Delta\psi_{mt}$ is the mitochondrial homeostatic center, the assessment of $\Delta\psi_{mt}$ in cells is worth investigating. Our experimental data showed that cells treated with **6f**-UVA exhibited a marked decrease in $\Delta\psi_{mt}$. A drop in $\Delta\psi_{mt}$ promotes the opening of the permeability transition (PT), which leads to mitochondrial dysfunction. Moreover, mitochondrial oxidative phosphorylation is the major ATP synthetic pathway in eukaryotes. A study is in progress to investigate whether decreased intracellular ATP is due to **6f**-UVA treatment. Our study showed a

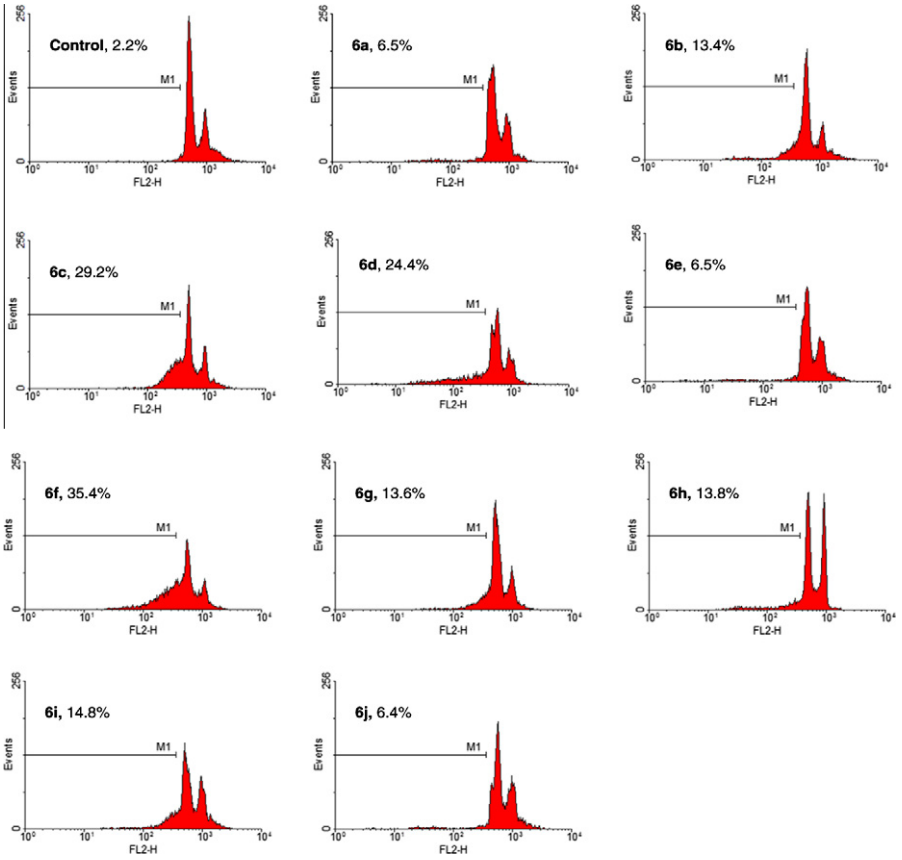

Figure 3. Effect of compound tested on the cellular sub-G1 content. BCC cells were treated with 4 μM agents for 4 h followed by 1 J/cm^2 UVA. Twenty four hours after irradiation, the PI reagent was used. Approximately 10,000 cells from each group were analyzed with the FACScan flow cytometer. Data represent the percentage of cell counts and display sub-G1.

decrease of intracellular ATP content in response to **6f**-UVA treatment.

Owing to studies suggesting that the activity of the MAPKs after PDT are suspected to be of importance in the process of cell death,[24–26] this prompted us to investigate whether MAPK-signaling pathways were involved in **6f**-UVA-induced apoptosis. Our study showed that **6f**-UVA caused apoptosis in parallel with the activation of ERK and p38 in BCC cells. Although PDT has been shown to activate JNK with different photosensitizers,[24,27] **6f**-UVA did not affect the JNK-P expression, indicating that JNK MAPK is not involved in **6f**-UVA-induced apoptosis. The preceding results demonstrate that mitochondria and MAPK participate in apoptosis of BCC cells. Nevertheless, the possible interrelationships among these substances in **6f**-UVA-induced apoptosis are not clear. Thus, we investigated whether the ERK activation correlated with alterations in ATP levels. Cells were pretreated with oligomycin or ATP before **6f**-UVA treatment. Our result showed that increased ERK phosphorylation was caused by reduced cellular ATP synthesis.

The data gathered in this study demonstrate that cells exposed to **6f**-UVA initiate mitochondrial changes including an increased ROS generation, a decline in $\Delta\psi_{mt}$, and a reduction of ATP. In addition, **6f**-UVA treatment also induced ERK and p38 MAPK phosphorylation. We propose that **6f**-UVA treatment induces cell apoptosis through the mitochondrial pathway, which subsequently activates p38 and ERK. In the present article, we describe the effect of UVA-activated **6** on BCC cells in vitro. Our findings suggest that **6** have photosensitive activity for BCC cells. Further studies are required to elucidate the precise mechanism of the photosensitive effect of **6** in vivo at the molecular biological level.

4. Experimental

4.1. Syntheses

Chemical reagents were obtained without further purification. Solvents free distillated prior to use. Reactions were monitored by thin layer chromatography, using Merck plates 60 F_{254}. Flash chromatography was carried out on Merck Silica Gel 60 (40–63 μm) using the indicated solvents. Melting points were determined using Fargo MP-2D and are uncorrected. ^{1}H NMR and ^{13}C NMR spectra were recorded on Varian UNITY plus-400 at 400 and 100 MHz, respectively, using $CDCl_3$ as a solvent. ^{1}H NMR chemical shifts are referenced to TMS or $CDCl_3$ (7.26 ppm). ^{13}C NMR was referenced to $CDCl_3$ (77.0 ppm). Mass spectra were recorded with Bruker APEX II spectrometer. Elemental analyses were performed on Elementar vario EL III analyzer, and the results were found to be ±0.4% of the theoretical values. Purity of tested compounds was >95%.

4.1.1. General procedure for the syntheses of benzamides (3a–3f) (method a)

To a stirred solution of aniline (225 mmol, 1.2 equiv) in pyridine (450 mL) was added 4-nitrobenxzoyl chloride (186 mmol) under nitrogen at room temperature, then the mixture was refluxed for 4 h. After being cooled to room temperature, the solution was poured into ice/water. The resulting precipitate was filtered and recrystallized from methylene chloride to give the corresponding compounds **3**.

4.1.1.1. 4-Nitro-*N*-phenylbenzamide 3a. White solid; 91% yield; mp 214–216 °C; ^{1}H NMR ($CDCl_3$, 400 MHz) δ 9.42 (br s, NH), 8.38

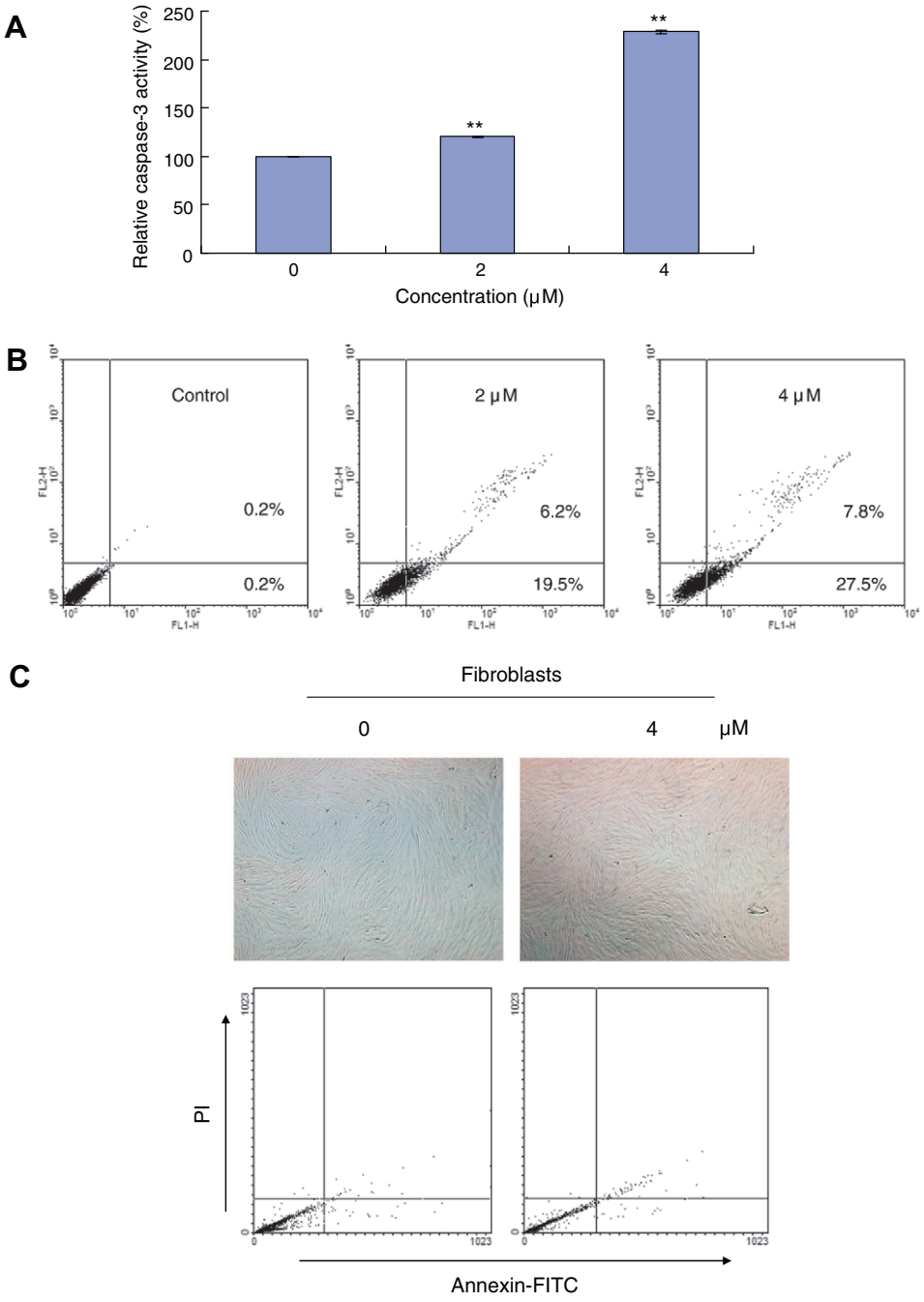

Figure 4. Effect of **6f**-UVA treatment on cell apoptosis. (A) The increased enzymatic activities of the caspase-3 in apoptotic were determined by colorimetric reaction. The cleavage of peptide by the caspase releases the chromophore pNA (*p*-nitroaniline), which can be quantified spectrophotometrically at a wavelength of 405 nm. (B) Dot plots for BCC cells treated with various concentrations of **6f**-UVA and then stained with PI and an annexin V-FITC conjugate specifically detecting the exposure of PS residues at the cell surface. (C) Morphological observation and annexin V/PI double stain were used for the detection of fibroblasts apoptosis. Approximately 10,000 cells from each group were analyzed by flow cytometry. Data shown are of a representative experiment repeated three times with similar results. $^{**}p$ <0.01 as compared with the control.

(dt, J = 2.4 and 3.6 Hz, 2H), 8.23 (dt, J = 2.4 and 3.6 Hz, 2H), 7.85–7.82 (m, 2H), 7.40–7.35 (m, 2H), 7.17–7.13 (m, 1H); ^{13}C NMR ($CDCl_3$, 100 MHz) δ 165.3, 151.2, 142.6, 140.5, 130.5, 130.3, 125.8, 125.1, 121.8; HRMS (EI, *m/z*) for $C_{13}H_{10}N_2O_3$ calcd 242.0691, found 242.0692. Anal. Calcd for $C_{13}H_{10}N_2O_3$: C, 64.46; H, 4.16; N, 11.56. Found: C, 64.72; H, 4.25; N, 11.54.

4.1.1.2. *N*-(4-Methylphenyl)-4-nitrobenzamide 3b. White solid; 93% yield; mp 201–203 °C; ^{1}H NMR ($CDCl_3$, 400 MHz) δ 9.37 (br s, NH), 8.26 (d, J = 8.8 Hz, 2H), 8.11 (d, J = 8.4 Hz, 2H), 7.58 (d, J = 8.0 Hz, 2H), 7.16 (d, J = 8.0 Hz, 2H), 2.34 (s, 3H); ^{13}C NMR ($CDCl_3$, 100 MHz) δ 163.8, 149.3, 140.7, 135.3, 134.4, 129.3, 128.7, 123.4, 120.8, 20.8; HRMS (ESI, *m/z*) for $C_{14}H_{12}N_2O_3Na$ calcd 279.0746, found 279.0744. Anal. Calcd for $C_{14}H_{12}N_2O_3$: C, 65.62; H, 4.72; N, 10.93. Found: C, 65.71; H, 5.00; N, 10.92.

4.1.1.3. *N*-(4-Ethylphenyl)-4-nitrobenzamide 3c. White solid; 96% yield; mp 186–188 °C; ^{1}H NMR ($CDCl_3$, 400 MHz) δ 8.32 (dd, J = 5.2 and 1.6 Hz, 2H), 8.03 (d, J = 8.4 Hz, 2H), 7.92 (br s, NH), 8.23 (d, J = 8.0 Hz, 2H), 7.22 (d, J = 8.4 Hz, 2H), 2.65 (q, J = 7.6 Hz, 2H), 1.24 (t, J = 7.2 Hz, 3H); ^{13}C NMR ($CDCl_3$, 100 MHz) δ 163.6, 149.6, 141.5, 140.6, 134.8, 128.6, 128.2, 124.0, 120.6, 28.4, 15.6;

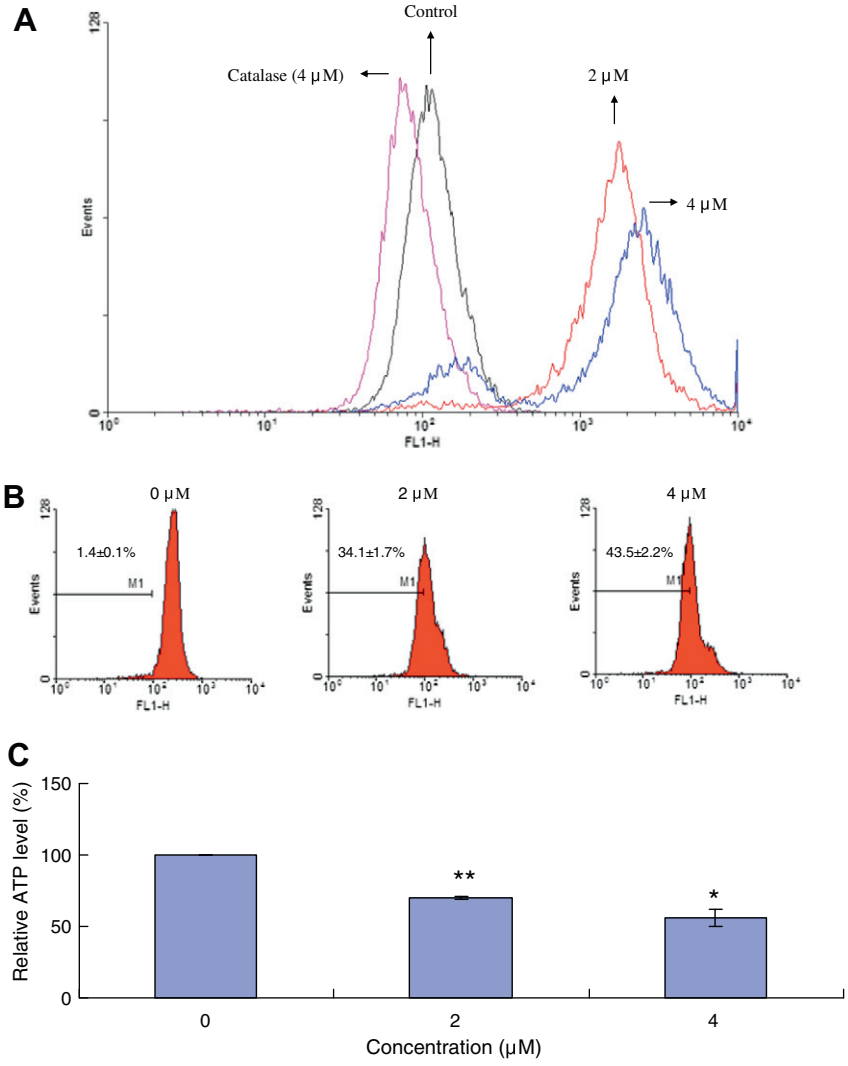

Figure 5. Effect of **6f**-UVA on the mitochondrial function. (A) **6f**-UVA induced ROS generation in BCC cells. Histogram of fluorescence vs cell count in BCC cells with various concentrations of **6f**-UVA and stained with DCFH-DA. As a control, ROS was measured in the presence of catalase, a H_2O_2 scavenger. (B) The $\Delta\psi_{mt}$ of BCC cells after exposure to **6f**-UVA. Cells were treated with 0, 2, and 4 μM **6f** for 4 h followed by 1 J/cm^2 UVA irradiation, then stained with $DiOC_6$ and analyzed immediately by flow cytometry as described under Section 4. The number in M1 indicates the percentage of cells with reduced $\Delta\psi_{mt}$. Approximately 10,000 cells from each group were analyzed by flow cytometry. (C) Relative ATP levels were calculated as the percentage of the 0 μM level. Similar results were obtained in three independent experiments. $^*p$ <0.05, $^{**}p$ <0.01 as compared with the control.

HRMS (ESI, *m/z*) for $C_{15}H_{15}N_2O_3$ calcd 271.1083, found 271.1084. Anal. Calcd for $C_{15}H_{14}N_2O_3$:C, 66.66; H, 5.22; N, 10.36. Found: C, 66.48; H, 5.41; N, 10.15.

4.1.1.4. *N*-(3-Methoxyphenyl)-4-nitrobenzamide 3d. Yellow solid; 80% yield; mp 158–160 °C; ^{1}H NMR ($CDCl_3$, 400 MHz) δ 9.98 (br s, NH), 8.31–8.28 (m, 2H), 8.18 (d, J = 8.8 Hz, 2H), 7.94 (s, 1H), 7.32–7.23 (m, 2H), 6.72–6.69 (m, 1H), 3.82 (s, 3H); ^{13}C NMR ($CDCl_3$, 100 MHz) δ 163.8, 159.5, 149.0, 140.5, 139.2, 129.1, 128.7, 123.0, 112.8, 109.9, 106.3, 54.9; HRMS (ESI, *m/z*) for $C_{14}H_{12}N_2O_4Na$ calcd 295.0695, found 295.0694. Anal. Calcd for $C_{14}H_{12}N_2O_4$: C, 61.76; H, 4.44; N, 10.29. Found: C, 61.49; H, 4.59; N, 10.33.

4.1.1.5. *N*-(4-Methoxyphenyl)-4-nitrobenzamide 3e. Yellow solid; 80% yield; mp 196–197 °C; ^{1}H NMR ($CDCl_3$, 400 MHz) δ 9.35 (br s, NH), 8.22 (d, J = 8.0 Hz, 2H), 8.07 (d, J = 8.0 Hz, 2H), 7.68 (d, J = 8.4 Hz, 1H), 6.95 (d, J = 8.4 Hz, 2H), 3.75 (s, 3H); ^{13}C NMR ($CDCl_3$, 100 MHz) δ 163.7, 156.6, 149.2, 140.7, 130.9, 128.6, 123.3, 122.5, 113.9, 55.3; HRMS (ESI, *m/z*) for $C_{14}H_{13}N_2O_4$ calcd 273.0875, found 273.0873. Anal. Calcd for $C_{14}H_{12}N_2O_4$: C, 61.76; H, 4.44; N, 10.29. Found: C, 61.88; H, 4.65; N, 10.14.

4.1.1.6. *N*-(4-Trifluoromethylphenyl)-4-nitrobenzamide 3f. White solid; 95% yield; mp 194–196 °C; ^{1}H NMR (DMSO, 400 MHz) δ 10.87 (br s, NH), 8.37 (d, J = 8.4 Hz, 2H), 8.14 (d, J = 8.4 Hz, 2H), 7.97 (d, J = 8.0 Hz, 2H), 7.70 (d, J = 8.4 Hz, 2H); ^{13}C NMR (DMSO, 100 MHz) δ 164.9, 149.6, 142.5, 140.3, 129.6, 126.3, 124.5 (q, J = 140 Hz, 1C), 123.9, 120.7, 114.1; HRMS (EI, *m/z*) for $C_{14}H_9F_3N_2O_3$ calcd 310.0560, found 310.0563. Anal. Calcd for $C_{14}H_9F_3N_2O_3$: C, 54.20; H, 2.92; N, 9.03. Found: C, 54.50; H, 2.84; N, 9.25.

4.1.2. General procedure for the syntheses of benzamides (3g–3j) (method b)

To a stirred solution of 4-nitrobenzoic acid (82 mmol) in benzene (165 mL) was treated with thionyl chloride (58 mL, 820 mmol, 10 equiv) under nitrogen at room temperature then the mixture was reflux for 4 h. After removal of solvent, the benzoyl chloride intermediate was added slowly to a solution of the appropriately substituted aniline (123 mmol, 1.5 equiv) in pyridine

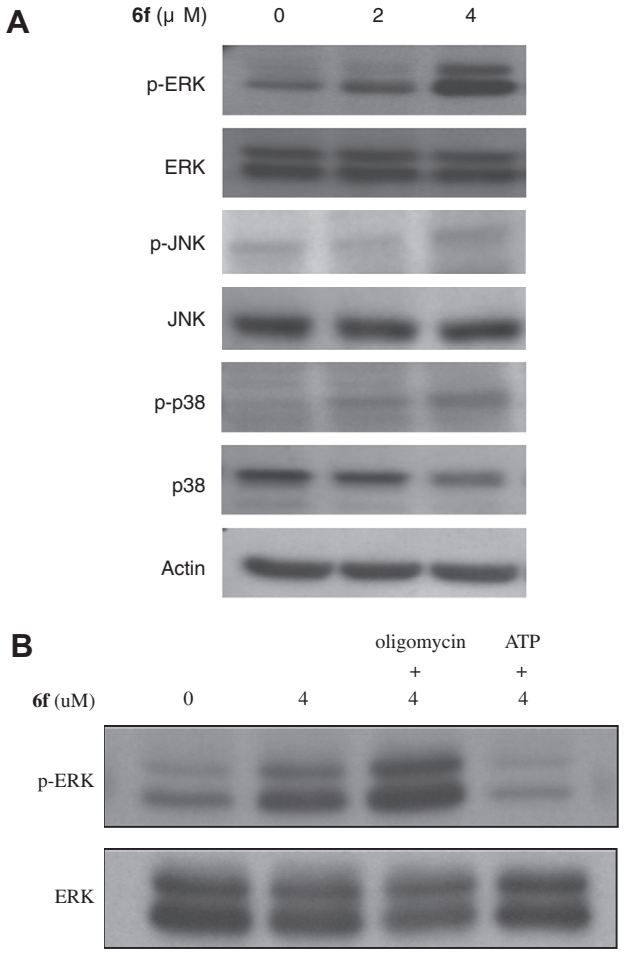

Figure 6. Immunoblot analysis showed the effect of **6f**-UVA on the protein expression of MAP kinases on BCC cells. (A) After exposure to different concentration of **6f**-UVA, cell lysates were collected and immunoblotted with specific antibodies as indicated. For the internal control, the same amounts of protein extract were also probed with antibody against actin. (B) As a control, the expression level of *p*-ERK was determined in the presence of oligomycin (25 μM) and ATP (1×10^{-4} M).

(165 mL). The mixture was refluxed under nitrogen at room temperature for 4 h. After being cooled room temperature, the solution was poured into ice/water. The resulting precipitate was filtered and recrystallized from methylene chloride to give the corresponding compounds **3**.

4.1.2.1. *N*-(Phenyl)-3-methyl-4-nitrobenzamide 3g. White solid; 82% yield; mp 149–151 °C; ^{1}H NMR ($CDCl_3$, 400 MHz) δ 8.01 (d, J = 8.4 Hz, 1H), 7.98 (br s, NH), 7.84 (s, 1H), 7.78 (d, J = 8.4 Hz, 1H), 7.63 (d, J = 7.6 Hz, 2H), 7.40–7.36 (m, 2H), 7.21–7.17 (m, 1H), 2.64 (s, 3H); ^{13}C NMR ($CDCl_3$, 100 MHz) δ 163.9, 150.9, 138.8, 137.27, 134.2, 131.8, 139.2, 125.4, 125.3, 125.0, 120.4, 20.3; HRMS (ESI, *m/z*) for $C_{14}H_{13}N_2O_3$ calcd 257.0926, found 257.0925. Anal. Calcd for $C_{14}H_{12}N_2O_3$: C, 65.62; H, 4.72; N, 10.93. Found: C, 65.53; H, 4.60; N, 11.00.

4.1.2.2. *N*-(4-Ethylphenyl)-3-methyl-4-nitrobenzamide 3h. White solid; 80% yield; mp 137–139 °C; ^{1}H NMR ($CDCl_3$, 400 MHz) δ 8.03 (br s, NH), 7.97 (d, J = 8.4 Hz, 1H), 7.82 (s, 1H), 7.75 (d. J = 8.4 Hz, 1H), 7.52 (d, J = 8.4 Hz, 2H), 7.29 (d, J = 8.0 Hz, 2H), 2.67–2.61 (m, 5H), 1.24 (t, J = 8.4 Hz, 3H); ^{13}C NMR ($CDCl_3$, 100 MHz) δ 163.8, 150.8, 141.4, 138.9, 134.9, 134.1, 131.8, 128.5, 125.4, 125.0, 120.6, 28.3, 20.3, 15.6; HRMS (ESI, *m/s*) for $C_{16}H_{17}N_2O_3$ calcd 285.1239, found 285.1241. Anal. Calcd for $C_{16}H_{16}N_2O_3$: C, 67.59; H, 5.67; N, 9.85. Found: C, 67.50; H, 5.45; N, 9.85.

4.1.2.3. *N*-(4-Methoxyphenyl)-3-methyl-4-nitrobenzamide 3i. White solid; 71% yield; mp 152–154 °C; ^{1}H NMR ($CDCl_3$, 400 MHz) δ 7.98 (d, J = 8.4 Hz, 1H), 7.94 (br s, NH), 7.81 (s, 1H), 7.75 (d. J = 8.0 Hz, 1H), 7.52 (d, J = 8.8 Hz, 2H), 6.89 (d, J = 9.2 Hz, 2H), 3.81 (s, 3H), 2.62 (s, 3H); ^{13}C NMR ($CDCl_3$, 100 MHz) δ 163.7, 157.0, 150.8, 138.8, 134.1, 131.7, 130.2, 125.3, 124.9, 122.3, 114.3, 114.2, 55.4, 20.2; HRMS (ESI, *m/z*) for $C_{15}H_{15}N_2O_4$ calcd 287.1032, found 287.1033. Anal. Calcd for $C_{15}H_{14}N_2O_4$: C, 62.93; H, 4.93; N, 9.79. Found: C, 62.77; H, 5.17; N, 9.82.

4.1.2.4. 3-Methyl-4-nitro-*N*-(4-trifluoromethyl-phenyl)benzamide 3j. White solid; 75% yield; mp 154–156 °C; ^{1}H NMR ($CDCl_3$, 400 MHz) δ 9.38 (br s, NH), 8.01 (d, J = 8.8 Hz, 1H), 7.92 (s, 1H), 7.87–7.83 (m, 2H), 7.61 (d, J = 8.4 Hz, 2H), 2.64 (s, 3H); ^{13}C NMR ($CDCl_3$, 100 MHz) δ 164.8, 150.8, 141.0, 138.4, 133.8, 132.1, 126.1 (q, J = 38 Hz, CF_3–C), 125.8, 124.7, 123.2 (q, J = 140 Hz, CF_3), 120.3, 120.2 20.0; HRMS (EI, *m/z*) for $C_{15}H_{11}N_2O_2F_3$ calcd 324.0722, found 324.0725. Anal. Calcd for $C_{15}H_{11}F_3N_2O_3$: C, 55.56; H, 3.42; N, 8.64. Found: C, 55.50; H, 3.48; N, 8.64.

4.1.3. General procedure for the syntheses of thiobenzamide (4a–4j)

A mixture of the substituted 4-nitro-*N*-phenylbenzamide (41 mmol) and Lawesson's reagent (8.52 g?21 mmol, 0.51 equiv) in chlorobenzene (30 mL) was heated at reflux for 4–6 h, after which it was concentrated, purified by column chromatography (CH_2Cl_2/hexane = 2:3) to give the corresponding compounds **4**.

4.1.3.1. 4-Nitro-*N*-phenylthiobenzamide 4a. Yellow solid; 60% yield; mp 154–156 °C; ^{1}H NMR ($CDCl_3$, 400 MHz) δ 9.08 (br s, NH), 8.26 (d, J = 8.4 Hz, 2H), 7.95 (d, J = 8.4 Hz, 2H), 7.77 (d, J = 7.6 Hz, 2H), 7.47 (t, J = 8.0 Hz, 2H), 7.34 (t, J = 8.0 Hz, 1H); ^{13}C NMR ($CDCl_3$, 100 MHz) δ 195.5, 148.9, 148.2, 138.5, 129.2, 127.7, 127.5, 123.9, 123.5; HRMS (EI, *m/z*) for $C_{13}H_{10}N_2O_2S$ calcd 258.0463, found 258.0463. Anal. Calcd for $C_{13}H_{10}N_2O_2S$, C, 60.45; H, 3.90; N, 10.85. Found: C, 60.44; H, 4.06; N, 10.75.

4.1.3.2. *N*-(4-Methylphenyl)-4-nitrothiobenzamide 4b. Yellow solid; 60% yield; mp 195–196 °C; ^{1}H NMR ($CDCl_3$, 400 MHz) δ 9.15 (br s, NH), 8.21 (d, J = 8.4 Hz, 2H), 7.91 (d, J = 8.8 Hz, 2H), 7.60 (d, J = 8.4 Hz, 2H), 7.26–7.23 (m, 2H), 2.38 (s, 3H); ^{13}C NMR ($CDCl_3$, 100 MHz) δ 195.27, 148.8, 148.0, 137.6, 135.9, 129.7, 127.7, 123.8, 123.6, 21.2; HRMS (ESI, *m/z*) for $C_{14}H_{12}N_2O_2SNa$ calcd 295.0517, found 295.0516. Anal. Calcd for $C_{14}H_{12}N_2O_2S$: C, 61.75; H, .4.44; N, 10.29. Found: C, 61.81; H, 4.55; N, 10.29.

4.1.3.3. *N*-(4-Ethylphenyl)-4-nitrothiobenzamide 4c. Yellow solid; 65% yield; mp 142–144 °C; ^{1}H NMR ($CDCl_3$, 400 MHz) δ 9.07 (br s, NH), 8.25 (d, J = 8.4 Hz, 2H), 7.94 (d, J = 8.8 Hz, 2H), 7.66 (d, J = 8.4 Hz, 2H), 7.28 (d, J = 8.0 Hz, 2H), 2.69 (q, J = 8.0 Hz 2H), 1.27 (t, J = 7.6 Hz, 3H); ^{13}C NMR ($CDCl_3$, 100 MHz) δ 195.2, 148.9, 148.2, 143.9, 136.1, 128.9, 128.6, 127.7, 123.9, 123.5, 28.5, 15.3; HRMS (ESI, *m/z*) for $C_{15}H_{15}N_2O_2S$ calcd 287.0854, found 287.0856. Anal. Calcd for $C_{15}H_{14}N_2O_2S$: C, 62.92; H, .4.93; N, 9.78. Found: C, 62.91; H, 4.95; N, 9.60.

4.1.3.4. *N*-(3-Methoxyphenyl)-4-nitrothiobenzamide 4d. Yellow solid; 64% yield; mp 138–140 °C; ^{1}H NMR ($CDCl_3$, 400 MHz) δ 10.61 (br s, NH), 8.23 (d, J = 8.8 Hz, 2H), 7.96 (d, J = 8.8 Hz, 2H), 7.60 (s, 1H), 7.36–7.30 (m, 2H), 6.86–6.83 (m, 1H), 3.83 (s, 3H); ^{13}C NMR ($CDCl_3$, 100 MHz) δ 195.3, 159.8, 148.8, 148.2, 146.2, 129.6, 128.2, 123.3, 115.8, 112.7, 109.2, 55.4; HRMS (ESI, *m/z*) for $C_{14}H_{12}N_2O_3SNa$ calcd 311.0466, found 311.0464. Anal. Calcd for

$C_{14}H_{12}N_2O_3S$: C, 58.32; H, .4.20; N, 9.72. Found: C, 58.25; H, 4.36; N, 9.61.

4.1.3.5. *N*-(4-Methoxyphenyl)-4-nitrothiobenzamide 4e. Yellow solid; 62% yield; mp 174–175 °C; ^{1}H NMR ($CDCl_3$, 400 MHz) δ 9.98 (br s, NH), 8.31–8.28 (m, 2H), 8.18 (d, J = 8.8 Hz, 2H), 7.94 (s, 1H), 7.32–7.23 (m, 2H), 6.72–6.69 (m, 1H), 3.82 (s, 3H); ^{13}C NMR ($CDCl_3$, 100 MHz) δ 163.8, 159.5, 149.0, 140.5, 139.2, 129.1, 128.7, 123.0, 112.8, 109.9, 106.3, 54.85; HRMS (EI, *m/z*) for $C_{14}H_{12}N_2O_3S$ calcd 288.0569, found 288.0571. Anal. Calcd for $C_{14}H_{12}N_2O_3S$: C, 58.32; H, .4.20; N, 9.72. Found: C, 58.29; H, 4.42; N, 9.47.

4.1.3.6. *N*-(4-Trifluoromethylphenyl)-4-nitrothiobenzamide 4f. Yellow solid; 71% yield; mp 174–175 °C; ^{1}H NMR ($CDCl_3$, 400 MHz) δ 11.49 (br s, NH), 8.25 (d, J = 8.4 Hz, 2H), 8.07 (d, J = 8.8 Hz, 2H), 7.99 (d, J = 8.4 Hz, 2H), 7.68 (d, J = 8.0 Hz, 2H); ^{13}C NMR ($CDCl_3$, 100 MHz) δ 196.1, 148.5, 148.0, 142.4, 128.4, 125.8, 125.8, 123.5, 123.1, 122.3 (q, J = 140 Hz, CF_3); HRMS (ESI, *m/z*) for $C_{14}H_{10}N_2O_2F_3S$ calcd 326.0337, found 326.0335. Anal. calcd for $C_{14}H_{10}N_2O_2F_3S$: C, 51.53; H, 2.78; N, 8.59. Found: C, 51.90; H, 2.86; N, 8.63.

4.1.3.7. *N*-(Phenyl)-3-methyl-4-nitrothiobenzamide 4g. Yellow solid; 72% yield; mp 118–120 °C; ^{1}H NMR ($CDCl_3$, 400 MHz) δ 9.09 (br s, NH), 7.99 (d, J = 8.4 Hz, 1H), 7.78–7.71 (m, 4H), 7.46 (t, J = 8.0 Hz, 2H), 7.33 (t, J = 7.6 Hz, 1H), 2.64 (s, 3H); ^{13}C NMR ($CDCl_3$, 100 MHz) δ 195.7, 146.6, 138.5, 134.2, 131.2, 129.2, 127.4, 125.1, 124.8, 123.5, 20.5; HRMS (ESI, *m/z*) for $C_{14}H_{13}N_2O_2S$ calcd 273.0698, found 273.0700. Anal. Calcd for $C_{14}H_{13}N_2O_2S$: C, 61.75; H, 4.44; N, 10.29. Found: C, 62.01; H, 4.39; N, 10.26.

4.1.3.8. *N*-(4-Ethylphenyl)-3-methyl-4-nitrothiobenzamide 4h. Yellow solid; 70% yield; mp 160–162 °C; ^{1}H NMR ($CDCl_3$, 400 MHz) δ 9.03 (br s, NH), 7.99 (d, J = 8.4 Hz, 1H), 7.78–7.65 (m, 3H), 7.28 (d, J = 8.4 Hz, 2H), 2.72–2.64 (m, 5H), 1.26 (t, J = 7.6 Hz, 3H); ^{13}C NMR ($CDCl_3$, 100 MHz) δ 195.4, 150.1, 146.6, 143.8, 136.1, 134.2, 131.3, 128.5, 125.0, 124.81 123.5, 28.5, 20.5, 15.4; HRMS (ESI, *m/z*) for $C_{16}H_{17}N_2O_2S$ calcd 301.1011, found 301.1012. Anal. Calcd for $C_{16}H_{17}N_2O_2S$: C, 63.98; H, 5.37; N, 9.33. Found: C, 63.99; H, 5.39; N, 9.30.

4.1.3.9. *N*-(4-Methoxyphenyl)-3-methyl-4-nitrothiobenzamide 4i. Yellow solid; 61% yield; mp 160–162 °C; ^{1}H NMR ($CDCl_3$, 400 MHz) δ 10.81 (br s, NH), 7.96 (d, J = 8.1 Hz, 1H), 7.83 (dd, J = 1.6 and 0.8 Hz, 1H), 7.77 (dd, J = 8.4 and 2.0 Hz, 1H), 7.69 (dt, J = 8.8 and 3.2 Hz, 2H), 6.94 (dt, J = 8.8 and 3.2 Hz, 2H), 3.83 (s, 3H), 2.63 (s, 3H); ^{13}C NMR ($CDCl_3$, 100 MHz) δ 195.0, 157.9, 149.5, 146.2, 133.3, 132.2, 131.7, 125.4, 124.3, 113.7, 55.2, 20.2; HRMS (ESI, *m/z*) for $C_{15}H_{15}N_2O_3S$ calcd 303.0803, found 303.0804. Anal. Calcd for $C_{15}H_{15}N_2O_3S$: C, 59.59; H, 4.67; N, 9.27. Found: C, 59.95; H, 4.90; N, 9.07.

4.1.3.10. 3-Methyl-4-nitro-*N*-(4-trifluoromethylphenyl)thiobenzamide 4j. Yellow solid; 74% yield; mp 170–172 °C; ^{1}H NMR ($CDCl_3$, 400 MHz) δ 8.04–7.98 (m, 3H), 7.81–7.68 (m, 4H), 2.65 (s, 3H); ^{13}C NMR ($CDCl_3$, 100 MHz) δ 208.5, 196.6, 149.8, 146.4, 142.2, 133.5, 131.5, 125.8, 125.3, 124.4, 123.5, 122.3 (q, J = 140 Hz, CF_3), 29.7, 20.0; HRMS (ESI, *m/z*) for $C_{15}H_{11}N_2O_2SF_3$ calcd 340.0493, found 340.0494. Anal. Calcd for $C_{15}H_{11}N_2O_2SF_3$: C, 52.94; H, 3.26; N, 8.23. Found: C, 52.68; H, 3.47; N, 8.27.

4.1.4. General procedure for the syntheses of 2-(4-nitrophenyl)-benzothiazole (5a–5j)

A solution of substituted 4-nitrothiobenzamides (50 mmol) in three drops of 95% EtOH and 30% aqueous sodium hydroxide solution (10.6 mL, 8 equiv) was added dropwise to a solution of potassium ferricyanide (13.16 g, 4 equiv) in water (50 mL) at 90 °C. The reaction mixture was heated for a further 1 h and then cooled in ice. The resulting precipitate was filtered and washed with water, then subjected to flash chromatography (CH_2Cl_2/hexane = 1:4) to give the corresponding compounds **5**.

4.1.4.1. 2-(4-Nitrophenyl)benzothiazole 5a. White solid; 68% yield; mp 228–230 °C; ^{1}H NMR ($CDCl_3$, 400 MHz) δ 8.35 (dt, J = 9.2 and 2.0 Hz, 2H), 8.27 (dt, J = 9.2 and 2.0 Hz, 2H), 8.13 (d, J = 8.0 Hz, 1H), 7.96 (d, J = 8.0 Hz, 1H), 7.56 (dt, J = 8.0 and 1.2 Hz, 1H), 7.47 (dt, J = 8.0 and 1.2 Hz, 1H); ^{13}C NMR ($CDCl_3$, 100 MHz) δ 164.8, 154.1, 149.0, 139.1, 135.4, 128.2, 126.9, 126.2, 124.3, 123.9, 121.8; HRMS (EI, *m/z*) for $C_{13}H_8N_2O_2S$ calcd 256.0306, found 256.0308. Anal. Calcd for $C_{13}H_8N_2O_2S$: C, 60.93; H, 3.15; N, 10.93. Found: C, 60.89; H, 3.34; N, 10.75.

4.1.4.2. 6-Methyl-2-(4-nitrophenyl)benzothiazole 5b. White solid; 65% yield; mp 148–150 °C; ^{1}H NMR ($CDCl_3$, 400 MHz) δ 8.31 (s, 1H), 8.23 (s, 2H), 7.99 (d, J = 6.4 Hz, 1H), 7.72 (s, 1H), 7.36 (s, 1H), 2.52 (s, 3H); ^{13}C NMR ($CDCl_3$, 100 MHz) δ 163.7, 152.2, 148.8, 139.3, 136.6, 135.6, 128.5, 128.0, 124.2, 123.3, 121.4, 21.6; HRMS (EI, *m/z*) for $C_{14}H_{12}N_2O_2S$ calcd 295.0517, found 295.0516. Anal. Calcd for $C_{14}H_{10}N_2O_2S$: C, 62.21; H, 3.73; N, 10.36. Found: C, 62.37; H, 3.91; N, 10.31.

4.1.4.3. 6-Ethyl-2-(4-nitrophenyl)benzothiazole 5c. White solid; 72% yield; mp 151–152 °C; ^{1}H NMR ($CDCl_3$, 400 MHz) δ 8.34 (dd, J = .8 and 2.0 Hz, 2H), 8.25 (dd, J = 4.8 and 2.0 Hz, 2H), 8.02 (d, J = 8.4 Hz, 1H), 7.76 (d, J = 0.8 Hz, 1H), 7.40 (dd, J = 8.4 and 1.6 Hz, 1H), 2.28 (q, J = 7.6 Hz, 2H), 1.33 (t, J = 7.6 Hz, 3H); ^{13}C NMR ($CDCl_3$, 100 MHz) δ 163.8, 152.4, 148.8, 143.0, 139.3, 135.7, 128.0, 127.6, 124.3, 123.5, 120.3, 29.0, 15.7; HRMS (ESI, *m/z*) for $C_{15}H_{12}N_2O_2S$ calcd 285.0698, found 285.0695. Anal. Calcd for $C_{15}H_{12}N_2O_2S$: C, 63.36; H, 4.25; N, 9.85. Found: C, 63.40; H, 4.55; N, 9.53.

4.1.4.4. 7-Methoxy-2-(4-nitrophenyl)benzothiazole 5d. White solid; 25% yield; mp 228–230 °C; ^{1}H NMR ($CDCl_3$, 400 MHz), δ 8.33 (d, J = 8.8 Hz, 2H), 8.25 (d, J = 8.8 Hz, 2H), 7.75–7.73 (m, 1H), 7.49 (t, J = 8.4 Hz, 1H), 6.89 (d, J = 8.4 Hz, 1H), 4.03 (s, 3H); ^{13}C NMR ($CDCl_3$, 100 MHz) δ 165.4, 155.6, 154.3, 148.9, 139.2, 128.2, 127.8, 124.3, 116.4, 105.9, 56.0; HRMS (ESI, *m/z*) for $C_{14}H_{10}N_2O_3S$-Na calcd 309.0310, found 309.0308. Anal. Calcd for $C_{14}H_{10}N_2O_3S$: C, 58.73; H, 3.52; N, 9.78. Found: C, 58.94; H, 3.70; N, 9.65.

4.1.4.5. 6-Methoxy-2-(4-nitrophenyl)benzothiazole 5e. Yellow solid; 63% yield; mp 214–216 °C; ^{1}H NMR ($CDCl_3$, 400 MHz) δ 8.33 (dt, J = 9.2 and 2.0 Hz, 2H), 8.20 (dt, J = 9.2 and 2.0 Hz, 2H), 8.00 (d, J = 9.2 Hz, 1H), 7.38 (d, J = 2.4 Hz, 1H), 7.15 (dd, J = 9.2 and 2.4 Hz, 1H), 3.92(s, 3H); ^{13}C NMR ($CDCl_3$, 100 MHz) δ 162.2, 158.5, 148.7, 148.6, 139.3, 137.0, 127.8, 124.5, 124.2, 116.6, 104.0, 55.8; HRMS (ESI, *m/z*) for $C_{14}H_{11}N_2O_3S$ calcd 287.0490, found 287.0492. Anal. calcd for $C_{14}H_{10}N_2O_3S$: C, 58.73; H, 3.52; N, 9.78. Found: C, 58.68; H, 3.47; N, 9.75.

4.1.4.6. 2-(4-Nitrophenyl)-6-trifluoromethyl-benzothiazole 5f. Yellow solid; 61% yield; mp 149–151 °C; ^{1}H NMR ($CDCl_3$, 400 MHz) δ 8.35 (dt, J = 9.2 and 2.0 Hz, 2H), 8.27–8.23 (m, 3H), 8.19 (d, J = 8.4 Hz, 1H), 7.77 (dd, J = 8.4 and 2.0 Hz, 1H); ^{13}C NMR ($CDCl_3$, 100 MHz) δ 167.8, 155.8, 149.4, 138.3, 135.4, 128.4, 128.2, 124.3, 124.2, 123.9, 123.8, 119.5; HRMS (ESI, *m/z*) for $C_{14}H_7N_2O_2SF_3$ calcd 324.0175, found 324.0178. Anal. Calcd for $C_{14}H_7N_2O_2SF_3$: C, 51.85; H, 2.18; N, 8.64. Found: C, 51.86; H, 2.22; N, 8.69.

4.1.4.7. 2-(3-Methyl-4-nitrophenyl)benzothiazole 5g. White solid; 71% yield; mp 163–165 °C; ^{1}H NMR ($CDCl_3$, 400 MHz) δ 8.13–8.08 (m, 3H), 8.02 (dd, J = 8.0 and 2.0 Hz, 1H), 7.95 (dd, J = 8.0 and

1.2 Hz, 1H), 7.55 (dt, J = 8.0 and 1.2 Hz, 1H), 7.45 (dt, J = 8.0 and 1.2 Hz, 1H), 2.71 (s, 3H); ^{13}C NMR ($CDCl_3$, 100 MHz) δ 165.1, 153.9, 150.1, 137.4, 135.4, 134.7, 131.4, 126.8, 126.0, 125.8, 125.5, 123.7, 121.8, 20.6; HRMS (ESI, m/z) for $C_{14}H_{11}N_2O_2S$ calcd 271.0541, found 271.0541. Anal. calcd for $C_{14}H_{11}N_2O_2S$: C, 62.21; H, 3.73; N, 10.36. Found: C, 62.07; H, 3.88; N, 10.26.

4.1.4.8. 6-Ethyl-2-(3-methyl-4-nitrophenyl)benzothiazole 5h.

Yellow solid; 75% yield; mp 118–120 °C; ^{1}H NMR ($CDCl_3$, 400 MHz) δ 8.10 (d, J = 8.8 Hz, 1H), 8.08 (s, 1H), 8.02 (d, J = 8.4 Hz, 1H), 8.01 (dd, J = 8.4 and 2.0 Hz, 1H), 7.75 (d, J = 2.0 Hz, 1H), 7.38 (dd, J = 8.4 and 2.0 Hz, 1H), 2.83 (q, J = 7.6 Hz, 2H), 2.71 (s, 3H), 1.33 (t, J = 7.6 Hz, 3H); ^{13}C NMR ($CDCl_3$, 100 MHz) δ 164.1, 152.4, 149.9, 142.8, 137.7, 135.6 134.6, 131.3, 127.4, 125.6, 125.5, 123.3, 120.3, 29.0, 20.6, 15.7; HRMS (ESI, m/z) for $C_{16}H_{15}N_2O_2S$ calcd 299.0854, found 299.0856. Anal. Calcd for $C_{16}H_{15}N_2O_2S$: C, 64.41; H, 4.73; N, 9.39. Found: C, 64.20; H, 4.80; N, 9.14.

4.1.4.9. 6-Methoxy-2-(3-methyl-4-nitrophenyl)benzothiazole 5i.

Yellow solid; 64% yield; mp 195–197 °C; ^{1}H NMR ($CDCl_3$, 400 MHz) δ 8.07 (d, J = 8.8 Hz, 1H), 8.02 (d, J = 0.8 Hz, 1H), 7.98 (d, J = 9.2 Hz, 1H), 7.95 (dd, J = 8.4 and 2.0 Hz, 1H), 7.36 (d, J = 2.4 Hz, 1H), 7.14 (dd, J = 9.2 and 2.4 Hz, 1H), 3.90 (s, 3H), 2.71 (s, 3H); ^{13}C NMR ($CDCl_3$, 100 MHz) δ 162.3, 158.4, 149.6, 148.6, 137.6, 136.8, 134.6, 130.9, 125.5, 125.3, 124.3, 116.4, 103.9, 55.8, 20.6; HRMS (ESI, m/z) for $C_{15}H_{14}N_2O_3S$ calcd 301.0647, found 301.0648. Anal. calcd for $C_{15}H_{14}N_2O_3S$: C, 59.93; H, 4.03; N, 9.33. Found: C, 60.37 H, 4.13; N, 9.36.

4.1.4.10. 2-(3-Methyl-4-nitrophenyl)-6-trifluoromethylbenzothiazole 5j.

Yellow solid; 30% yield; mp 99–101 °C; ^{1}H NMR ($CDCl_3$, 400 MHz) δ 8.21–8.15 (m, 2H), 8.08–8.06 (m, 2H), 8.00 (dd, J = 8.8 and 1.6 Hz, 1H), 7.76 (dd, J = 8.8 and 1.6 Hz, 1H), 2.69 (s, 3H); ^{13}C NMR ($CDCl_3$, 100 MHz) δ 168.0, 155.7, 150.4, 136.6, 135.2 134.6, 131.60, 127.9 (q, J = 32.6 Hz, 1C), 125.9 (d, J = 43.2 Hz, 1C), 125.49, 124.08, 123.8, 122.2, 119.4 (q, J = 4.5 Hz, 1C), 20.4; HRMS (ESI, m/z) for $C_{15}H_{10}N_2O_2F_3S$ calcd 339.0415, found 339.0414. Anal. Calcd for $C_{15}H_9N_2O_2F_3S$: C, 53.25; H, 2.68; N, 8.28. Found: C, 53.21; H, 2.73; N, 8.14.

4.1.5. General procedure for the syntheses of 2-(4-aminophenyl)-benzothiazole (6a–6j)

To a solution of 2-(4-nitrophenyl)benzothiazole (1 g, 3.9 mmol) in CH_2Cl_2 (30 mL) was added 10%Pd/C (0.1 g) under hydrogen at room temperature for 4 h. The resulting solution was concentrated and subjected to flash chromatography (CH_2Cl_2) to give the corresponding compounds **6**.

4.1.5.1. 2-(4-Aminophenyl)benzothiazole 6a.

Yellow solid; 94% yield; mp 130–132 °C; ^{1}H NMR ($CDCl_3$, 400 MHz) δ 7.99 (m, 1H), 7.89 (m, 2H), 7.84 (m, 1H), 7.44 (m, 1H), 7.32 (m, 1H), 6.72 (dt, J = 4.2 and 2.0 Hz, 2H), 4.00 (br s, NH_2); ^{13}C NMR ($CDCl_3$, 100 MHz) δ 168.5, 154.2, 149.2, 134.6, 129.1, 126.0, 124.4, 123.9, 122.5, 121.4, 114.8; HRMS (ESI, m/z) for $C_{13}H_{10}N_2S$ calcd 226.0565, found 226.0567. Anal. Calcd for $C_{13}H_{10}N_2S$: C, 69.00; H, 4.45; N, 12.38. Found: C, 69.01; H, 4.69; N, 12.29.

4.1.5.2. 2-(4-Aminophenyl)-6-methylbenzothiazole 6b.

Yellow solid; 95% yield; mp 181–183 °C; ^{1}H NMR ($CDCl_3$, 400 MHz) δ 7.88–7.85 (m, 3H), 7.63 (s, 1H), 7.25 (dd, J = 6.8 and 1.6 Hz, 1H), 6.71 (dd, J = 4.4 and 2.4 Hz, 1H), 7.32 (m, 1H), 6.72 (dt, J = 4.2 and 2.0 Hz, 2H), 4.00 (br s, NH_2), 2.46 (s, 3H); ^{13}C NMR ($CDCl_3$, 100 MHz) δ 167.5, 152.3, 149.0, 134.7, 134.5, 129.5, 129.0, 127.6, 126.3, 124.1, 122.0, 121.2, 114.8, 21.5; HRMS (ESI, m/z) for $C_{14}H_{13}N_2S$ calcd 241.0799, found 241.0798. Anal. Calcd for $C_{14}H_{12}N_2S$: C, 69.97; H, 5.03; N, 11.66. Found: C, 69.84; H, 5.01; N, 11.70.

4.1.5.3. 2-(4-Aminophenyl)-6-ethylbenzothiazole 6c.

Yellow solid; 92% yield; mp 154–156 °C; ^{1}H NMR ($CDCl_3$, 400 MHz) δ 7.90–7.86 (m, 3H), 7.65 (t, J = 0.4 Hz, 1H), 7.27 (dd, J = 7.6 and 2.0 Hz, 1H), 6.81 (dt, J = 4.8 and 2.0 Hz, 2H), 3.98 (br s, NH_2), 2.76 (q, J = 7.6 Hz, 2H), 1.29 (t, J = 7.6 Hz, 3H); ^{13}C NMR ($CDCl_3$, 100 MHz) δ 167.6, 152.5, 149.0, 141.0, 134.7, 129.0, 126.5, 124.1, 122.1, 114.7, 28.87, 15.8; HRMS (ESI, m/z) for $C_{15}H_{14}N_2OSNa$ calcd 277.0775, found 277.0776. Anal. calcd for $C_{15}H_{14}N_2S$: C, 70.83; H, 5.55; N, 11.01. Found: C, 70.62; H, 5.29; N, 10.90.

4.1.5.4. 2-(4-Aminophenyl)-7-methoxybenzothiazole 6d.

Yellow solid; 95% yield; mp 142–144 °C; ^{1}H NMR ($CDCl_3$, 400 MHz) δ 7.90 (d, J = 8.4 Hz, 2H), 7.62 (d, J = 8.0 Hz, 1H), 7.39 (t, J = 8.0 Hz, 1H), 6.78 (d, J = 8.0 Hz, 1H), 6.73 (d, J = 8.4 Hz, 2H), 3.99 (s, 5H); ^{13}C NMR ($CDCl_3$, 100 MHz) δ 169.1, 15.9, 154.2, 149.2, 129.1, 126.9, 124.0, 123.0, 115.3, 114.8, 104.7, 55.9; HRMS (ESI, m/z) for $C_{14}H_{13}N_2OS$ calcd 257.0749, found 257.0748. Anal. Calcd for $C_{14}H_{12}N_2OS$: C, 65.60; H, 4.72; N, 10.93. Found: C, 65.66; H, 4.86; N, 10.92.

4.1.5.5. 2-(4-Aminophenyl)-6-methoxybenzothiazole 6e.

Yellow solid; 96% yield; mp 174–176 °C; ^{1}H NMR ($CDCl_3$, 400 MHz) δ 7.88 (s, 1H), 7.84 (dt, J = 4.8 and 2.8 Hz, 2H), 7.32 (d, J = 2.4 Hz, 1H), 7.04 (dd, J = 4.8 and 2.4 Hz, 1H), 7.73 (dt, J = 4.8 and 2.8 Hz, 2H), 3.98 (br s, NH_2), 3.87 (s, 3H); ^{13}C NMR ($CDCl_3$, 100 MHz) δ 166.1, 157.3, 148.8, 148.8, 135.9, 135.9, 128.8, 124.2, 123.0, 115.1, 114.8, 104.3, 55.8; HRMS (ESI, m/z) for $C_{14}H_{13}N_2OS$ calcd 257.0749, found 257.0748. Anal. Calcd for $C_{14}H_{12}N_2OS$: C, 65.60; H, 4.72; N, 10.93. Found: C, 65.35; H, 4.90; N, 10.67.

4.1.5.6. 2-(4-Aminophenyl)-6-trifluoromethylbenzothiazole 6f.

Yellow solid; 91% yield; mp 181–183 °C; ^{1}H NMR ($CDCl_3$, 400 MHz) δ 8.11 (s, 1H), 8.03 (d, J = 8.4 Hz, 1H), 7.90 (dt, J = 4.8 and 2.4 Hz, 2H), 7.67 (dd, J = 6.8 and 1.6 Hz, 1H), 6.73 (dt, J = 4.8 and 2.4 Hz, 2H), 4.08 (br s, NH_2); ^{13}C NMR ($CDCl_3$, 100 MHz) δ 169.9, 158.1, 149.9, 132.3, 129.4, 123.1, 123.0, 122.5, 119.0, 119.0, 114.7; HRMS (ESI, m/z) for $C_{14}H_9F_3N_2S$ calcd 294.0439, found 294.0438. Anal. Calcd for $C_{14}H_9F_3N_2S$: C, 57.14; H, 3.08; N, 9.52. Found: C, 57.20; H, 3.18; N, 9.49.

4.1.5.7. 2-(4-Amino-3-methylphenyl)benzothiazole 6g.

Yellow solid; 94% yield; mp 147–149 °C; ^{1}H NMR ($CDCl_3$, 400 MHz) δ 7.99 (d, J = 8.0 Hz, 1H), 7.85–7.83 (m, 2H), 7.75 (dd, J = 8.0 and 2.0 Hz, 1H), 7.44 (td, J = 8.0 and 1.2 Hz, 1H), 7.31 (td, J = 8.0 and 1.2 Hz, 1H), 6.71 (d, J = 8.0 Hz, 1H), 3.94 (br s, NH_2), 2.23 (s, 3H); ^{13}C NMR ($CDCl_3$, 100 MHz) δ 168.7, 154.2, 147.5, 134.5, 129.7, 126.9, 126.0, 124.3, 123.8, 122.4, 122.1, 121.3, 114.5, 17.1; HRMS (ESI, m/z) for $C_{14}H_{12}N_2OSNa$ calcd 263.0619, found 263.0618. Anal. Calcd for $C_{14}H_{12}N_2OS$: C, 69.97; H, 5.03; N, 11.66. Found: C, 69.84; H, 5.01; N, 11.70.

4.1.5.8. 2-(4-Amino-3-methylphenyl)-6-ethylbenzothiazole 6h.

Yellow solid; 93% yield; mp 171–173 °C; ^{1}H NMR ($CDCl_3$, 400 MHz) δ 7.90 (d, J = 8.4 Hz, 1H), 7.80 (d, J = 1.6 Hz, 1H), 7.32 (dd, J = 6.0 and 2.4 Hz, 1H), 7.65 (d, J = 0.8 Hz, 1H), 7.27 (dd, J = 6.8 and 1.6 Hz, 1H), 6.70 (d, J = 8.4 Hz, 1H), 3.92 (br s, NH_2), 2.76 (q, J = 8.0 Hz, 2H), 2.22 (s, 3H), 1.29 (t, J = 7.6 Hz, 3H); ^{13}C NMR ($CDCl_3$, 100 MHz) δ 167.8, 152.5, 147.4, 140.9, 140.9, 134.7, 129.6, 126.8, 126.5, 124.1, 122.1, 122.0, 120.0, 114.6, 28.9, 17.2, 15.8; HRMS (ESI, m/z) for $C_{16}H_{17}N_2OS$ calcd 269.1112, found 269.1110. Anal. Calcd for $C_{16}H_{16}N_2S$: C, 71.61; H, 6.01; N, 10.44. Found: C, 72.01; H, 6.36; N, 10.52.

4.1.5.9. 2-(4-Amino-3-methylphenyl)-6-methoxybenzothiazole 6i. Yellow solid; 95% yield; mp 151–153 °C; ^{1}H NMR ($CDCl_3$, 400 MHz) δ 7.87 (d, J = 8.8 Hz, 1H), 7.77 (d, J = 2.0 Hz, 1H), 7.69 (dd, J = 6.0 and 2.4 Hz, 1H), 7.30 (d, J = 2.8 Hz, 1H), 7.03 (dd, J = 6.0 and 2.4 Hz, 1H), 6.69 (d, J = 8.4 Hz, 1H), 3.86 (s, 5H), 2.22 (s, 3H); ^{13}C NMR ($CDCl_3$, 100 MHz) δ 166.4, 157.2, 148.7, 147.2, 135.8, 129.4, 126.6, 124.0, 122.9, 122.2, 115.0, 114.6, 104.3, 55.8, 17.2; HRMS (ESI, m/z) for $C_{15}H_{15}N_2OS$ calcd 271.0905, found 271.0906. Anal. Calcd for $C_{15}H_{14}N_2OS$: C, 66.64; H, 5.22; N, 10.36. Found: C, 66.68; H, 5.38; N, 10.48.

4.1.5.10. 2-(4-Amino-3-methylphenyl)-6-trifluoromethylbenzothiazole 6j. Yellow solid; 91% yield; mp 152–154 °C; ^{1}H NMR ($CDCl_3$, 400 MHz) δ 8.12 (s, 1H), 8.04 (d, J = 8.8 Hz, 1H), 7.83 (d, J = 1.2 Hz, 1H), 7.77 (dd, J = 6.0 and 2.4 Hz, 1H), 7.66 (dd, J = 6.8 and 1.6 Hz, 1H), 6.72 (d, J = 8 Hz, 1H), 4.20 (br s, NH_2), 2.24 (s, 3H); ^{13}C NMR ($CDCl_3$, 100 MHz) δ 171.1, 156.3, 148.3, 134.6, 130.0, 127.3, 126.4 (q, J = 65.5 Hz, 1C), 123.0 (q, J = 5.6 Hz, 1C), 122.4, 122.1, 118.9 (q, J = 5.6 Hz, 1C), 114.5, 17.2; HRMS (ESI, m/z) for $C_{15}H_{12}F_3N_2S$ calcd 308.0595, found 308.0597. Anal. Calcd for $C_{15}H_{11}F_3N_2S$: C, 58.43; H, 3.60; N, 9.09. Found: C, 58.50; H, 3.60; N, 9.09.

4.2. Cell culture

Fibroblasts were obtained from adult foreskin specimens as previously described[28] and human basal cell carcinoma (BCC), purchased from American Type Culture Collection (Manassas, VA), was maintained in RPMI1640 medium supplemented with 10% FCS and 100 U/mL penicillin G, and 100 μg/mL streptomycin sulfate (Gibco, BRL). BCC cells were passaged at confluence after treatment with 5 mM EDTA (Gibco, BRL) and incubated at 37 °C in a humidified atmosphere containing 5% CO_2.

4.3. UVA irradiation

The method for UVA irradiation was described in our previous study.[29] For UVA irradiation, a specific UVA lamp emitting a peak wavelength of 365 nm with intensity of 0.75 mW/cm^2 (Vilber Lourmat, Moune La Vallee, Cedex, France) was used. The cultured cells were pretreated with different agents at 4 μM or pretreated with various concentrations (0–4 μM) of **6** for 4 h before UVA irradiation. The cultured cells were rinsed with phosphate-buffered saline (PBS) and then irradiated with 1 J/cm^2 UVA in PBS to avoid the formation of medium-derived toxic photoproducts induced by UV exposure. The doses of irradiation were measured using a UVX radiometer (UVP, San Gabriel, CA, USA). Immediately after phototreatment, PBS was removed and media were added to the cells. All the following experiments were performed three times in triplicate.

4.4. Cell viability

Cell viability was assessed by the MTT assay, a mitochondrial function assay based on the ability of viable cells to reduce the redox indicator MTT to insoluble formazan crystals by mitochondrial dehydrogenase. Briefly, cells were seeded in a 96-well plate at the cell density of 2500 cells/well. After an overnight incubation, the cells were treated with compounds at 4 μM and incubated for 24 h. The medium was then discarded and replaced with 10 μL of MTT dye. Plates were incubated at 37 °C for 2 h. The resulting formazan crystals were solubilized in 100 μL DMSO, and the optical density was read at 540 nm with a microplate reader (MRX-II, Dynex technology, Chantilly, VA).

4.5. Sub-G1 region analysis

BCC cells were treated with compounds at 4 μM and 1 J/cm^2 UVA. Twenty-four hours after irradiation, cells were harvested by trypsinization and centrifugation. Cell pellets were resuspended in 50% cold ethanol and fixed at −20 °C. After fixation, cells were washed once with cold PBS and incubated in 0.5 mL of PBS containing 100 μg/mL RNase A for 20 min at 37 °C. Cells were harvested by centrifugation at 400g for 5 min, and 250 μL of PBS containing 50 μg/mL propidium iodide (PI) was added to the pellet. Thirty minutes later, the DNA contents of 10,000 events were measured by FACSscan flow cytometer (Elite ESP, Beckman Coulter, Brea, CA). Histograms were analyzed using Windows Multiple Document Interface software (WinMDI). Cells with DNA content less than that in untreated cells in G0/G1 were considered apoptotic.

4.6. Caspase-3 colorimetric assay

Twenty-four hours after irradiation, cells were collected by centrifugation, washed once with PBS, and cell pellets were counted and resuspended in 25 μL/1 × 10^6 cells of cold lysis buffer and homogenized. Homogenates were centrifuged at 12,000 rpm for 10 min at 4 °C, supernatants were used for measuring caspase-3 activity using an ELISA-based assay, according to the manufacturer's instructions (R&D Systems, Minneapolis, MN). The results were presented as mean ± SD.

4.7. Annexin V and PI binding assay

To assess the simultaneous observation of early phase of apoptotic and necrotic features, BCC cells were treated with various concentrations (0–4 μM) of **6f** for 4 h before irradiation. Twenty-four hours after irradiation, cells were harvested by trypsinization and centrifugation and measured by cytometry by adding annexin V-FITC to 10^6 cells per sample according to the manufacturer's specifications (Bender MedSystems, Vienna, Austria). Simultaneously, the cells were stained with PI. Flow cytometry data were analyzed by the WinMDI software.

4.8. Morphology observation

BCC or fibroblasts (5 × 10^5 cells/well) seeded on six well plate. Cells were treated with 4 μM **6f** for 4 h followed by 1 J/cm^2 UVA irradiation. Twenty four hours after exposure, take photos by using microscope at 200× phase.

4.9. Determination of intracellular ROS level

To evaluate intracellular reactive oxygen species (ROS) levels, 2′,7′-dichlorofluorescein diacetate (DCFH-DA, Molecular Probes) fluorescent dye was used to clarify this issue. The nonpolar DCFH-DA is converted to the polar derivative DCFH by esterases when it is taken up by the cell. DCFH is nonfluorescent but is rapidly oxidized to the highly fluorescent DCF by intracellular H_2O_2 or nitric oxide. In addition, catalase (Sigma), an effective H_2O_2 scavenger, was also used in this study. Cells were pretreated with catalase (800 U/mL) before **6f** (0–4 μM) treatment. After indicated irradiation, DCFH-DA (10 μM) was immediately added into cultured cells for 30 min at 37 °C. The fluorescence of the samples was measured with a flow cytometer. The 2′,7′-dichlorofluorescein (DCF) data were recorded using FL-1 photomultiplier.

4.10. Assessment of mitochondrial membrane potential ($\Delta\psi_{mt}$)

BCC cells were cultured in 35-mm dishes and allowed to reach exponential growth for 24 h before treatment. Cells were pre-

treated with 0, 2, and 4 μM **6f** for 4 h before 1 J/cm^2 UVA irradiation. The medium was removed and the adherent cells trypsinized. The cells were pelleted by centrifugation at 400*g* for 5 min and stained in a 100 nM/mL $DiOC_6$ dye (Molecular Probes, Eugene, OR) for 30 min at room temperature and washed with PBS twice and resuspended in PBS. The samples were analyzed immediately for fluorescence (FL-1 detector, filter 530/30 nm band pass) on a FACScan flow cytometer (Elite ESP, Beckman Coulter, Brea, CA). Histograms were analyzed using Windows Multiple Document interface software (WinMDI).

4.11. ATP content bioluminescence assay

The amount of intracellular ATP was determined by bioluminescent assay based on the measurement of the light output of the luciferin–luciferase reaction. After treatment with various concentrations of **6f**-UVA, total cell extracts from cultured BCC cells were obtained immediately by lysing solution. After centrifugation to remove cell debris, we collected supernatants for ATP measurement. The total amount of intracellular ATP was determined according to the protocol provided with the ATPLite assay kit (Perkin–Elmer, Boston, MA).

4.12. Protein extraction and western blot analysis

Total cell extracts from cultured BCC cells were obtained by lysing the cells in ice-cold RIPA buffer (1 × PBS, 1% NP-40, 0.5% sodium deoxycholate, 0.1% SDS) containing 100 μg/mL PMSF, 2 μg/mL aprotinin, 2 μg/mL leupeptin and 100 μg/mL NaF. After centrifugation at 14,000*g* for 30 min, protein in the supernatants was quantified by Bradford method (Bio-Rad). Forty micrograms of protein per lane was applied in 10% SDS–poly-acrylamide gel. After electrophoresis, protein was transferred from the gel to polyvinylidene difluoride (PVDF) membrane (Millipore, Bedford, MA). The membranes were blocked at room temperature for 1 h in PBS + 0.1% Tween 20 (PBS-T) containing 5% skim milk. After being briefly rinsed with PBS-T, the blots were probed with respective primary antibodies at room temperature for 2 h or at 4 °C overnight. Rabbit polyclonal antibodies against JNK (46 kDa), p38 (38 kDa), ERK (42, 44 kDa), and mouse monoclonal antibody against p-JNK, p-p38, p-ERK were purchased from Santa Cruz Biotechnology (Santa Cruz, CA). Mouse monoclonal antibody against actin was purchased from Chemicon Int. Inc. (Temecula, CA). For the blocking test, 25 μM oligomycin (Sigma, a mitochondria-specific F_0F_1 ATP synthase inhibitor) or 1×10^{-4} M ATP (Sigma) was added to the media 30 min before treated with **6f**-UVA, respectively. The membrane was incubated with the corresponding horseradish peroxidase-labeled secondary antibody (Santa Cruz Biotechnology) at room temperature for 1 h. Membranes were washed with PBS-T four times for 15 min, and the protein blots were visualized with Western Lightning Chemiluminescence Reagent Plus (Perkin–Elmer Life Sciences, Boston, MA). The relative amounts of specific proteins were quantified by densitometry scanning of X-ray films and analyzed by Eagle Eye Image System (Stratagene, La Jolla, CA).

4.13. Statistical analysis

The results were expressed as means ± SD and analyzed by using the statistical analysis system (SPSS, SPSS Inc., Chicago, IL). Differences among groups were analyzed by Student's *t*-test. *P* values <0.05 were considered as significant for all statistical tests.

Acknowledgments

We thank the National Science Council of the Republic of China, KMU Center of Excellence for Environmental Medicine (KMU-EM-97-2.1c), and Kaohsiung Medical University Research Foundation (KMU-M099014) for financial support.

Supplementary data

Supplementary data associated with this article can be found, in the online version, at doi:10.1016/j.bmc.2010.04.082.

References and notes

1. Neville, J. A.; Welch, E.; Leffell, D. J. *Nat. Clin. Pract. Oncol.* **2007**, *4*, 462.
2. Marks, R. *Cancer* **1995**, *75*, 607.
3. Grapengiesser, S.; Ericson, M.; Gudmundsson, F. *Clin. Exp. Dermatol.* **2002**, *27*, 493.
4. Morton, C. A.; Brown, S. B.; Collins, S. *Br. J. Dermatol.* **2002**, *146*, 552.
5. Morton, C. A.; MacKie, R. M.; Whitehurst, C. *Arch. Dermatol.* **1998**, *134*, 248.
6. Kiesslich, T.; Krammer, B.; Plaetzer, K. *Curr. Med. Chem.* **2006**, *13*, 2189.
7. Dolmans, D. E.; Fukumura, D.; Jain, R. K. *Cancer* **2003**, *3*, 380.
8. Shi, D.-F.; Bradshaw, T. D.; Wrigley, S.; McCall, C. J.; Lelieveld, P.; Stevens, M. F. G. *J. Med. Chem.* **1996**, *39*, 3375.
9. Bradshaw, T. D.; Wrigley, S.; Shi, D.-F.; Schultz, R. J.; Paull, K. D.; Stevens, M. F. G. *Br. J. Cancer* **1998**, *77*, 745.
10. Yates, P. C.; McCall, C. J.; Stevens, M. F. G. *Tetrahedron* **1991**, *47*, 6493.
11. Stevens, M. F. G.; McCall, C. J.; Lelieveld, P.; Alexander, P.; Richter, A.; Davies, D. E. *J. Med. Chem.* **1994**, *37*, 1689.
12. Gogvadze; Zhivotovsky, B. *J. Bioenerg. Biomembr.* **2007**, *39*, 23.
13. Crompton, M. *Biochem. J.* **1999**, *341*, 233.
14. Valencia, A.; Kochevar, I. E. *Free Radic. Biol. Med.* **2006**, *40*, 641.
15. Roulston, A.; Reinhard, C.; Amiri, P.; Williams, L. T. *J. Biol. Chem.* **1998**, *273*, 10232.
16. Nagata, Y.; Todokoro, K. *Blood* **1999**, *94*, 853.
17. Bacus, S. S.; Gudkov, A. V.; Lowe, M.; Lyass, L.; Yung, Y.; Komarov, A. P.; Keyomarsi, K.; Yarden, Y.; Seger, R. *Oncogene* **2001**, *202*, 147.
18. Xiao, D.; Singh, S. V. *Cancer Res.* **2002**, *62*, 3615.
19. Hutchinson, I.; Chua, M. S.; Browne, H. L.; Trapani, V.; Bradshaw, T. D.; Westwell, A. D.; Stevens, M. F. G. *J. Med. Chem.* **2001**, *44*, 1446.
20. Salvesen, G. S.; Dixit, V. M. *Cell* **1997**, *91*, 443–446.
21. Shi, Y. *Mol. Cell* **2002**, *9*, 459.
22. Hail, N., Jr. *Apoptosis* **2005**, *10*, 687.
23. Hildeman, D. A.; Mitchell, T.; Teague, T. K.; Henson, P.; Day, B. J.; Kappler, J.; Marrack, P. C. *Immunity* **1999**, *10*, 735.
24. Moor, A. C. *J. Photochem. Photobiol. B* **2000**, *57*, 1.
25. McCubrey, J. A.; Lahair, M. M.; Franklin, R. A. *Antioxid. Redox Signal.* **2006**, *8*, 1775.
26. Wong, T. W.; Tracy, E.; Oseroff, A. R.; Baumann, H. *Cancer Res.* **2003**, *63*, 3812.
27. Chan, W. H.; Yu, J. S.; Yang, S. D. *Biochem. J.* **2000**, *351*, 221.
28. Yang, C. C.; Lin, S. D.; Yu, H. S. *J. Dermatol. Sci.* **1997**, *14*, 162.
29. Kao, C. S.; Yu, H. S. *J. Invest. Dermatol.* **1992**, *98*, 734.